Parameter Identification and Modeling of Longitudinal Aerodynamics

J. W. Aksteter, E. K. Parks, R. E. Bach Jr.

Reprinted from

Journal of Aircraft

Volume 32, Number 4, Pages 726–731

AIAA

A publication of the
American Institute of Aeronautics and Astronautics, Inc.
370 L'Enfant Promenade, SW
Washington, DC 20024-2518

JOURNAL OF AIRCRAFT
Vol. 32, No. 4, July–August 1995

Parameter Identification and Modeling of Longitudinal Aerodynamics

J. W. Aksteter*
Science Applications International Corporation, California, Maryland 20619
E. K. Parks†
University of Arizona, Tucson, Arizona 85721
and
R. E. Bach Jr.‡
NASA Ames Research Center, Moffett Field, California 84035

Using a comprehensive flight test database and a parameter identification software program produced at NASA Ames Research Center, a math model of the longitudinal aerodynamics of the Harrier aircraft was formulated. The identification program employed the equation error method using multiple linear regression to estimate the nonlinear parameters. The formulated math model structure adhered closely to aerodynamic and stability/control theory, particularly with regard to compressibility and dynamic maneuvering. Validation was accomplished by using a three degree-of-freedom nonlinear flight simulator with pilot inputs from flight test data. The simulation models agreed quite well with the measured states. It is important to note that the flight test data used for the validation of the model was not used in the model identification.

Nomenclature

AR	=	aspect ratio
a_t	=	lift curve slope of the stabilator
a_x, a_y, a_z	=	inertial accelerations in body axis
$\boldsymbol{a}_i$, $\boldsymbol{b}_i$, $\boldsymbol{c}_i$	=	vectors of identified parameters
C_L, C_D, C_m	=	lift, drag, and pitching moment coefficients
C_{L_0}, C_{D_0}, C_{m_0}	=	lift, drag, and pitching moment regression constants
C_l	=	airfoil lift coefficient
$\bar{c}$	=	mean aerodynamic chord
e	=	Oswald's efficiency factor
F_x, F_y, F_z	=	total body axis forces
h	=	c.g. location, $\%\bar{c}$
h_n	=	neutral point location, $\%\bar{c}$
h_{ref}	=	reference c.g., $\%\bar{c}$
I	=	number of experimental observations
I_{xx}, I_{yy}, I_{zz}	=	body axis moments of inertia
I_{xz}	=	product of inertia
k	=	reduced frequency, $\omega\bar{c}/2V_T$
L	=	total rolling moment
l_t	=	lineal distance between aircraft c.g. and aerodynamic center of stabilator
M	=	total pitching moment
M_T	=	thrust-induced pitching moment
M_0	=	nominal Mach number
M_∞	=	freestream Mach number
$M_{\infty_{cr}}$	=	critical Mach number
m	=	mass
N	=	total yawing moment
p	=	roll rate
q	=	pitch rate
r	=	yaw rate
s	=	wing area
s_t	=	horizontal tail area
$\hat{q}$	=	dimensionless pitch rate, $q\bar{c}/2V_T$
U	=	x-body axis inertial velocity
V_H	=	horizontal tail volume ratio, $l_t S_t/\bar{c}S$
W	=	z-body axis velocity
X_T	=	x-body axis thrust
x_{ij}	=	matrix of experimental inputs
$\boldsymbol{Y}_i$	=	measured output vector
$\hat{\boldsymbol{Y}}_i$	=	estimated output vector
Z_T	=	z-body axis thrust
α	=	angle of attack
α_{stall}	=	stall angle of attack
α'	=	angle of attack marking onset of flow separation
$\dot{\alpha}$	=	rate of change of α
$\hat{\dot{\alpha}}$	=	dimensionless angle of attack rate, $\dot{\alpha}\bar{c}/2V_T$
δ_f	=	flap angle
δ_H	=	stabilator angle
δ_N	=	nozzle angle
ε	=	down wash angle
θ	=	pitch angle
Λ_{LE}	=	sweepback angle of wing leading edge
Λ_t	=	sweepback angle of horizontal tail leading edge
$\boldsymbol{\xi}_i$	=	vector of estimated model parameters
χ	=	normalized angle of attack
ω	=	input frequency

Received June 17, 1994; presented as Paper 94-2147 at the AIAA 7th Biennial Flight Test Conference, Colorado Springs, CO, June 20–23, 1994; revision received Dec. 9, 1994; accepted for publication Dec. 9, 1994.

*Aerospace Engineer, Simulation and Research Services Division, Systems Control Technology Group, 44417 Pecan Ct., Suite B. Member AIAA.

†Professor Emeritus, Department of Aerospace and Mechanical Engineering. Associate Fellow AIAA.

‡Aerospace Engineer, Guidance and Navigation Branch, M/S 210-9. Member AIAA.

Introduction

PARAMETER identification is a well-founded method of mathematical model development or improvement based on experimental data for which many sophisticated techniques exist. The underlying goal of each technique is to minimize the error between input and output data in a least-squares fashion. One method used quite successfully is the equation

error method where the error between some vector of output parameters and a vector of estimates based on some predetermined model structure is minimized. For example, given a model of the form

$$\hat{Y}_i = \xi_0 + \xi_1 x_{i1} + \xi_2 x_{i2} + \cdots + \xi_n x_{ij} \quad (1)$$

parameter identification using the equation error method estimates the parameters ξ_i by minimizing the least-squares error function

$$\sum_{i=1}^{I} (Y_i - \hat{Y}_i)^2$$

The reader is referred to Ref. 1 for the details in the application of this fundamental principal. This method is applied to the identification of a nonlinear mathematical model that describes the longitudinal aerodynamics of the YAV-8B vertical/short takeoff and landing (V/STOL) aircraft for a nozzles aft configuration with gear retracted and no stores.

Previous estimation models have also incorporated this method and met with great success.[2,3] One objective herein is the application of this method using a model structure that is derived from fundamental flight mechanics and aerodynamic theory rather than solely statistical considerations. Generally, a simpler and perhaps less cumbersome model will result.

A mathematical model of an aircraft can be instrumental in performance optimization studies, high-fidelity simulation, design enhancements and additions, control systems analyses, etc. Specifically, the culmination of this effort was slated for use in the implementation of an upgraded automatic control system.

This article begins with a summary of the data acquisition process. The second portion illustrates the formulation of a model structure based on basic aerodynamics pertaining to the dominant nonlinear effects at high angles of attack including compressibility. It summarizes the buildup of the short-period terms q and $\dot{\alpha}$, the latter of which being all but ignored in previous estimation models. A representation of the nonlinear flap terms is also introduced. Finally, the iterative steps required in the identification process are reviewed. The model is verified using a three degree-of-freedom simulation with thrust and stabilator values from flight test as the only inputs.

Data Acquisition

In order to obtain a database to be used in parameter estimation, significant planning was done so that the cycle of flight testing, data acquisition, and database generation was synthesized at the outset. This is a crucial step since a model can only be as good as the data used to derive it. Furthermore, maneuver selection is important since without appropriate inputs to the airframe, the aerodynamics are difficult to model due to the highly coupled nature of the system. In practice it is difficult to excite only the longitudinal dynamics independent of the lateral and vice versa. To this end, maneuvers were performed so as to minimize the action of one mode while maximizing the other. For example, to excite the longitudinal modes δ_f, δ_N and thrust were assumed constant as the pilot provided stick inputs through a series of maneuvers so as to maximize the variation in α, θ, q, etc., while minimizing the variation in the lateral states. A typical continuous maneuver at constant M_0 consisted of longitudinal stick doublets (two repetitions), a longitudinal frequency sweep, a 180-deg level turn, an angle-of-attack step (AOASTP), and a wind-up turn (WUP).

A fixed ground station was equipped with telemetry downlink and radar tracking systems. The telemetry data from the onboard system was downlinked and merged with radar data. A nose boom was mounted and equipped with α and sideslip vanes while all control surface positions were measured directly using displacement transducers. By disengaging the stability augmentation system and measuring the actual control surface deflections, configuration parameters, and engine operating parameters, the need to incorporate the reaction control system (RCS) into the modeling process was eliminated. Thus, the modeling is greatly simplified and strict attention may be placed on the fundamental aerodynamic phenomena, completely unobscured by complicated control algorithms. The inertial navigation system (INS) contained built-in rate gyros and accelerometers for measuring angular rates and linear accelerations. All onboard and telemetry data was sampled at a rate of 120 Hz for mainframe channels and 30 Hz for subframe channels. The reader is referred to Ref. 4 for further details.

The raw data files were processed using a smoothing and state-estimation program[5] incorporating the aircraft kinematical equations to estimate the states based on the appropriate data. It also checked for data consistency and provided estimates of useful unmeasured states such as the Euler angles and angular accelerations.

An engine model obtained from Ref. 2 was used off-line to provide engine forces and moments (including those produced by the RCS) at a reference point. The total measured body axis forces and moments are given by[4]

$$F_x = ma_x, \qquad F_y = ma_y, \qquad F_z = ma_z$$

$$L = I_{xx}\dot{p} + I_{xz}(a_z + pq) - (I_{yy} - I_{zz})qr$$

$$M = I_{yy}\dot{q} - I_{xz}(r^2 - p^2) - (I_{zz} - I_{xx})pr$$

$$N = -I_{zz}a_z - I_{xz}(\dot{p} - qr) - (I_{xx} - I_{yy})pq$$

where all of the inertial terms were computed by the engine model while the rates and accelerations were smoothed estimates of the data.

The flight test data was stored in a structured binary database that was arranged into separate 3–5 min test segments that collectively covered the flight envelope. The following nozzles aft subset was used for this work:

$$0.3 < M_\infty < 0.75$$

$$-5 \text{ deg} < \alpha < 18 \text{ deg}$$

$$5 \text{ deg} \le \delta_f \le 25 \text{ deg}$$

The processed data file was stored at a rate of 20 Hz.

Formulation of the Aerodynamic Model Structure

A model describing the aerodynamic forces and moments acting on any aircraft must be capable of approximating all flight characteristics including static and fully dynamic maneuvers. It must address all nonlinearities and also account for compressibility effects.

The general functional formulation of the lift, drag, and pitching moment coefficient models may be stated as shown in Eqs. (2) where C_{L_0}, C_{D_0}, and C_{m_0} are the values of C_L, C_D, and C_m, when all other terms are zero. The model assumes that thrust induced aerodynamic effects are negligible for Mach ≥ 0.3. It also assumes that the dynamic terms (i.e., q and $\dot{\alpha}$) and δ_H have negligible influence on C_D:

$$\begin{aligned} C_L &= C_{L_{\text{basic}}}(\alpha, M_\infty) + \Delta C_{L_{\delta_H}}(\delta_H, M_\infty) \\ &\quad + \Delta C_{L_q}(q, \delta_f) + \Delta C_{L_{\dot{\alpha}}}(\dot{\alpha}, \delta_f) + \Delta C_{L_{\delta_f}}(\alpha, \delta_f) \\ C_D &= C_{D_{\text{basic}}}(C_L, M_\infty) + \Delta C_{D_{\delta_f}}(C_L, \delta_f) \\ C_m &= C_{m_{\text{basic}}}(C_L, h_n) + \Delta C_{m_{\delta_H}}(\delta_H, M_\infty) \\ &\quad + \Delta C_{m_q}(q, \delta_f) + \Delta C_{m_{\dot{\alpha}}}(\dot{\alpha}, \delta_f) \end{aligned} \quad (2)$$

Each of the Eqs. (2) is to be rewritten in a form compatible for regression analysis.[1] To do so requires careful review of the data so that each term on the right-hand side (RHS) is formulated in such a way as to provide the appropriate incremental contribution.

Nonlinear Approximation of Lift

Since drag and pitching moment are strongly dependent upon lift, it becomes important to approximate the dominant nonlinearities through the lift model. For incompressible flow, the basic lift for any conventional fixed wing subsonic aircraft is generally a linear function of α up to some α', at which flow separation becomes appreciable and the relationship becomes nonlinear (e.g., $\partial^2 C_L/\partial\alpha^2|_{\alpha\geq\alpha'} < 0$). Based on static thin airfoil theory,[6] lift may be approximated as

$$C_l = 2\pi \sin\alpha \cong a_1\alpha + a_2\alpha^3 \qquad (0 \leq \alpha < \alpha_{\text{stall}}) \quad (3)$$

where α_{stall} is the static stall angle of attack and a_1, a_2 are parameters to be identified. The region $\alpha \geq \alpha_{\text{stall}}$ is beyond the scope of this article. Although Eq. (3) applies to symmetric airfoils, its structure proves to be useful for aircraft estimation.

Compressibility and Static Models

To account for compressibility effects the Prandtl–Glauert similarity transformation[7] may be extended to finite wings and, in particular, to swept-back wings by defining the normalized angle of attack as

$$\chi = \alpha/\sqrt{1 - M_\infty^2 \cos^2\Lambda_{\text{LE}}} \quad (4)$$

where the denominator is known as the Prandtl–Glauert parameter and $M_\infty \cos\Lambda_{\text{LE}}$ is the component of M_∞ perpendicular to the wing leading edge.

Figure 1 shows three sets of flight test data measured at three values of M_∞. This illustrates clearly the increase in C_{L_α} with M_∞. Figure 2 shows the same data after normalization. The data reduces to a line indicating that compressibility is fully represented. Replacing α in Eq. (3) with χ, $C_{L_{\text{basic}}}$ was defined as

$$C_{L_{\text{basic}}} = a_1\chi + a_2\chi^3 + C_{L_0} \quad (5)$$

Note, however, that the Prandtl–Glauert rule is only valid for small α (say $\alpha < 20$ deg for this aircraft) and for $M_\infty < M_{\infty_{\text{cr}}}$. Since the database included only data for which $M_\infty < 0.75$, locally sonic flow was of no concern.

The parabolic drag relationship

$$C_D = C_{D_0} + C_L^2/\pi Ae$$

was used as a starting point for the drag model. When the effects of compressibility were included via the Prandtl–Glauert similarity, the resulting basic drag model was defined as

$$C_{D_{\text{basic}}}(C_L, M_\infty) = b_1 C_L^2 + C_{D_0}/\sqrt{1 - M_\infty^2 \cos^2\Lambda_{\text{LE}}} \quad (6)$$

where b_1 and C_{D_0} are parameters to be identified.

Recall that C_{m_α} is always less than zero for a statically stable aircraft and is given by[8]

$$C_{m_\alpha} = (h - h_n)C_{L_\alpha}$$

This allows us to write the static pitching moment equation as

$$C_m = C_{m_0} + C_{m_\alpha}\alpha + C_{m_{\delta_H}}\delta_H$$
$$\cong C_{m_0} + (h - h_n)C_{L_{\text{basic}}} + C_{m_{\delta_H}}\delta_H$$

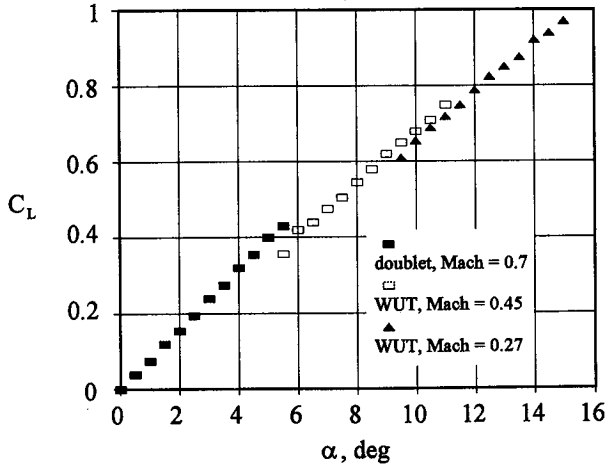

Fig. 1 Lift dependence on Mach number.

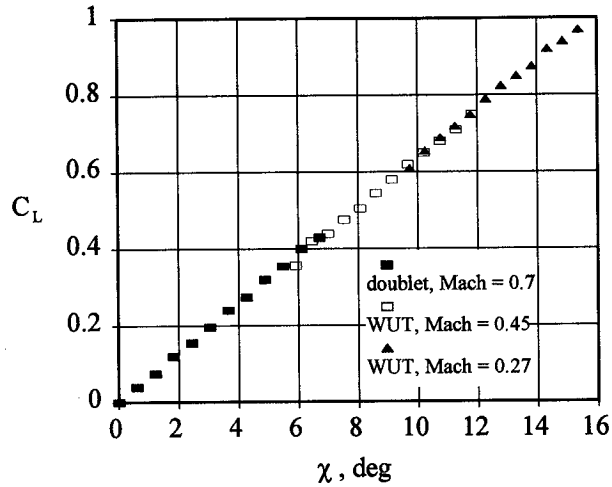

Fig. 2 Lift reduction using Prandtl–Glauert compressibility normalization.

where it is assumed that $h_n = h_n(\delta_f)$. Hence, $C_{m_{\text{basic}}}$ was defined as

$$C_{m_{\text{basic}}}(C_L, h_n) = c_1 C_{L_{\text{basic}}} + C_{m_0} \quad (7)$$

where c_1 and C_{m_0} are parameters to be identified.

The control terms in C_L and C_m were modeled as

$$\Delta C_{L_{\delta_H}}(\delta_H, M_\infty) = a_4\bar{\delta}_H$$
$$\Delta C_{m_{\delta_H}}(\delta_H, M_\infty) = c_3\bar{\delta}_H \quad (8)$$

where we account for compressibility effects of the stabilator as

$$\bar{\delta}_H = \delta_H/\sqrt{1 - M_\infty^2 \cos^2\Lambda_t}$$

Dynamic and Flap Increments

Any rotations about the c.g. will effect both the wing and tail in dynamic maneuvering. However, it is customary to assume that the wing contribution to ΔC_{L_q} and ΔC_{m_q} is negligible with respect to that of the tail. The same assumption holds true for $\Delta C_{L_{\dot\alpha}}$ and $\Delta C_{m_{\dot\alpha}}$ as well. Utilizing the approximate stability derivatives[8]

$$C_{L_{\dot\alpha}} = 2a_t V_H \frac{\partial\varepsilon}{\partial\alpha} = \frac{\partial\varepsilon}{\partial\alpha} C_{L_q}$$

$$C_{m_{\dot\alpha}} = -2a_t V_H \frac{l_t}{\bar{c}} \frac{\partial\varepsilon}{\partial\alpha} = \frac{\partial\varepsilon}{\partial\alpha} C_{m_q}$$

we may approximate the dynamical increments of Eqs. (2) as

$$\Delta C_{L_q} = C_{L_q}\hat{q}, \qquad \Delta C_{L_{\dot\alpha}} = C_{L_{\dot\alpha}}\hat{\dot\alpha}$$

$$\Delta C_{m_q} = C_{m_q}\hat{q}, \qquad \Delta C_{m_{\dot\alpha}} = C_{m_{\dot\alpha}}\hat{\dot\alpha}$$

Since q and $\dot\alpha$ are generally in phase and highly correlated with one another, it was useful to group these terms as

$$\Delta C_{L_q} + \Delta C_{L_{\dot\alpha}} = C_{L_q}\left(\hat{q} + \frac{\partial\varepsilon}{\partial\alpha}\hat{\dot\alpha}\right) = a_3\left(\hat{q} + \frac{\partial\varepsilon}{\partial\alpha}\hat{\dot\alpha}\right)$$
$$\Delta C_{m_q} + \Delta C_{m_{\dot\alpha}} = C_{m_q}\left(\hat{q} + \frac{\partial\varepsilon}{\partial\alpha}\hat{\dot\alpha}\right) = c_2\left(\hat{q} + \frac{\partial\varepsilon}{\partial\alpha}\hat{\dot\alpha}\right) \tag{9}$$

and identify C_{L_q} and C_{m_q} only (assuming $\partial\varepsilon/\partial\alpha \cong 0.65$), since highly correlated terms generally produce faulty identifications.

The inclusion of $\dot\alpha$ is essential. To understand the importance of this effect, consider a step input of δ_H that results in a response for which q and $\dot\alpha$ are roughly equivalent in both magnitude and phase. Conversely, a step input in α (i.e., a vertical gust) results in $\dot\alpha >> q$ over a small period of time. The model must include the $\dot\alpha$ terms in order to approximate the correct response.

Finally, the flap terms $\Delta C_{L_{\delta_f}}$ and $\Delta C_{D_{\delta_f}}$ were constructed by reviewing various sets of lift and drag data such as that shown in Figs. 3 and 4. Since these maneuvers were quasistatic (i.e., $\omega \to 0$), contributions from dynamic and control terms were negligible. Note from Fig. 3 that the conventional increment in C_L due to $\Delta\delta_f$ is evident but, more importantly, that there is a divergence of the three data sets for increasing α (or χ). To capture this nonlinearity, $\Delta C_{L_{\delta_f}}$ was defined as

$$\Delta C_{L_{\delta_f}}(\alpha, \delta_f) = a_5\delta_f + a_6\delta_f \tag{10}$$

Figure 4 shows a similar set of three quasistatic drag data segments where, in contrast, C_D converges for increasing values of C_L. This suggested that $\Delta C_{D_{\delta_f}}$ be defined as

$$\Delta C_{D_{\delta_f}}(C_L, \delta_f) = b_2\delta_f + b_3\delta_f C_L^2 \tag{11}$$

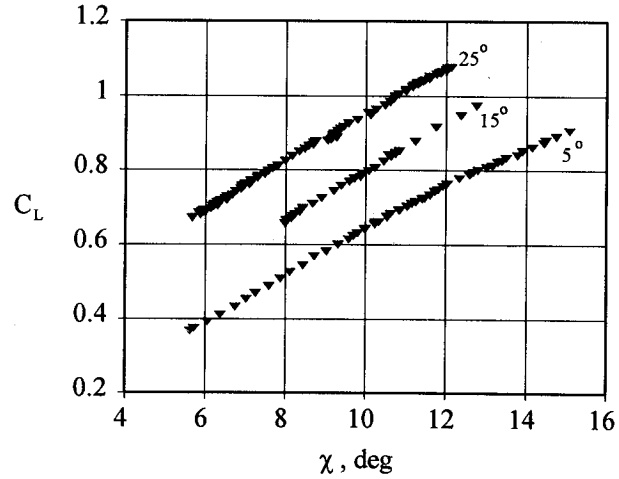

Fig. 3 Lift variation due to flaps (δ_f = 5, 15, and 25 deg).

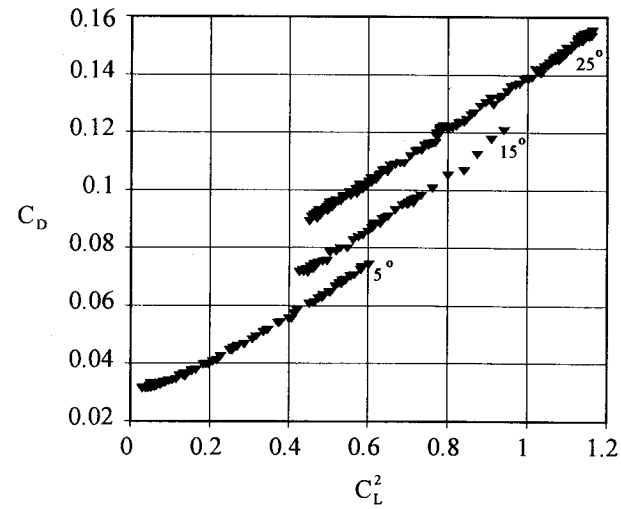

Fig. 4 Drag variation due to flaps (δ_f = 5, 15, and 25 deg).

Frequency Response Characteristics

The rigid body dynamic equations reveal that the states begin to attenuate when ω (the frequency of the δ_H in this case) approaches that of the short period. It was observed from flight test data that high-frequency rolloff occurred regularly during frequency sweep maneuvers for k exceeding ~0.06. In order to avoid erroneous identifications that would be prevalent due to negligible variance in the states relative to δ_H, data for which $k > 0.04$ was not used in the identification. A more detailed discussion of identifiability regions for aerodynamic parameters based on ω may be found in Ref. 9.

Results

Equations (5–11) were used to reformulate Eqs. (2) as

$$C_{L_{\text{model}}} = a_1\chi + a_2\chi^3 + a_3\left(\hat{q} + \frac{\partial\varepsilon}{\partial\alpha}\hat{\dot\alpha}\right) + a_4\bar{\delta}_H + a_5\delta_f + a_6\delta_f\alpha + C_{L_0}$$
$$C_{D_{\text{model}}} = b_1C_L^2 + b_2\delta_f + b_3\delta_f C_L^2 + C_{D_0}/\sqrt{1 - M_\infty^2\cos^2\Lambda_{\text{LE}}} \tag{12}$$
$$C_{m_{\text{model}}} = c_1C_L + c_2\left(\hat{q} + \frac{\partial\varepsilon}{\partial\alpha}\hat{\dot\alpha}\right) + c_3\bar{\delta}_H + C_{m_0}$$

The identification of the aerodynamic parameters utilized the equation error method to minimize the least-squared error between the modeled and measured coefficients. $C_{L_{\text{model}}}$, $C_{D_{\text{model}}}$, and $C_{m_{\text{model}}}$ were each identified separately. It was initially considered to identify Eqs. (12) simultaneously, but doing so may have inhibited the capability of distinguishing between the subtle effects inherent in flight dynamic modeling. By identifying each model separately, one may isolate the dominant vs negligible effects based primarily on physical rather than statistical characteristics.

In regression modeling of this nature, time chronology is not a factor in the selection of maneuvers since the regression model structure of Eqs. (12) is independent of time. Therefore, similar maneuvers from many different flights were concatenated in order to achieve the highest confidence in the results.

Identification Methodology

The model parameters were designated as static, dynamic, configuration, and/or control as illustrated in Table 1. Care was taken to identify the static terms using quasistatic data (i.e., data having frequencies k at or near the Phugoid frequency) at constant δ_f. In doing so, the dynamic, control, and configuration terms were fixed at reasonable values (based on theory and/or previous models) and the static terms were identified. The static terms were then fixed and the configuration terms were identified using quasistatic data with varying δ_f while keeping the a priori estimates of the dynamic and

Table 1 Parameter designation

a_1, a_2, b_1, c_1, C_{D_0}	Static
a_3, c_2	Dynamic
a_5, a_6, b_2, b_3, c_1, C_{L_0}, C_{m_0}	Configuration
a_4, c_3	Control

Table 2 Identified parameters

Parameter, (a_i, b_i, c_i)	$C_{L_{model}}$	$C_{D_{model}}$	$C_{m_{model}}$
1	4.456/rad	0.0776	$(h_{ref}{}^a - h_n)$
2	-8.394/rad^3	0.0421/rad	C_{m_q}
3	C_{L_q}	0.0470/rad	$C_{m_{\delta_H}}$
4	0.280/rad	——	——
5	0.774/rad^2	——	——
6	0.205/rad^2	——	——
$C_{L,D,m}\|_0$	~ -0.002	0.0225	$\sim$0.026

$h_n = 0.29 - 0.354\delta_f{}^b + 0.427\delta_f^2$
$C_{L_q} = 9.71\delta_f + 11.38$(/rad)
$C_{m_q} = 21.3\delta_f^2 - 0.6\delta_f - 13.8$(/rad)
$C_{m_{\delta_H}} = 1.4\delta_f - 1.8$(/rad)

[a] $h_{ref} = 0.1$. [b] δ_f is in units of radians.

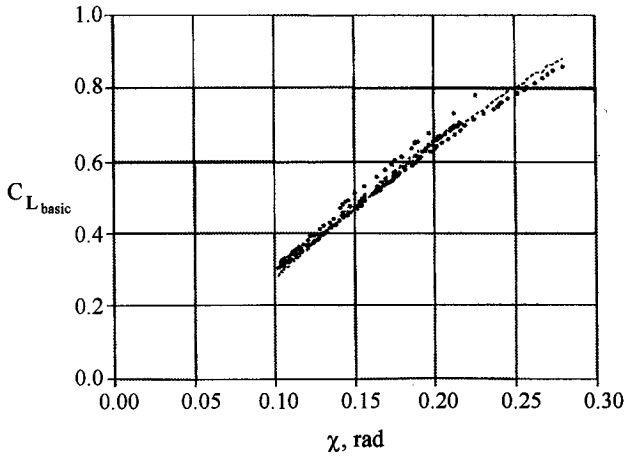

Fig. 5 Basic lift for $M_0 = 0.4$ (flight test data = symbols; model = dashed).

control terms. It was observed that c_1 required identification at different values of δ_f as it became evident that $h_n = h_n(\delta_f)$. The configuration terms were then fixed along with the static terms and the dynamic a priori estimates in order to identify the control terms. Finally, the configuration and control terms were fixed again and the process repeated until convergence was achieved. Since the dynamic terms were negligible relative to the others during quasistatic maneuvers, their a priori estimates had no appreciable influence on the static identification results.

Dynamic data (i.e., data having frequencies sufficiently larger than the Phugoid and at or below the short period) was used to identify the dynamic terms simultaneously with the control terms. Note that the control terms were identified from both quasistatic and dynamic data, the results of which show good agreement. Using dynamic data with varying δ_f showed that C_{L_q} and C_{m_q} (i.e., a_3 and c_2) were weak functions of δ_f. Having estimates of the dynamic terms based on the estimates of the static, configuration, and control terms, one iterative loop was complete. This iteration may be repeated as many times as needed for satisfactory convergence. Three was found to be sufficient.

Identified Math Model

Table 2 presents the identified parameters. The first column is the index number for the parameters a_i, b_i, and c_i to be

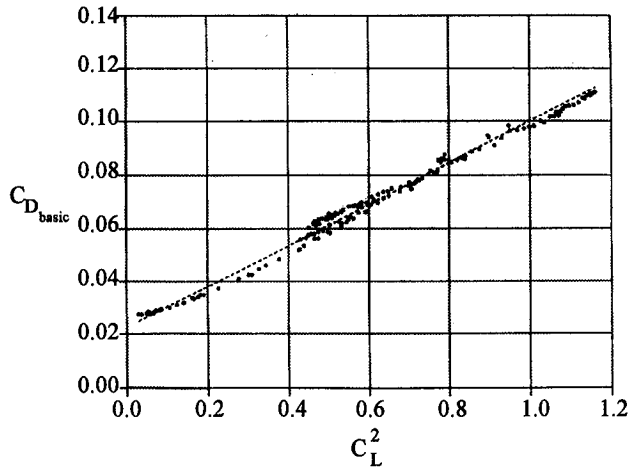

Fig. 6 Basic drag for $M_0 = 0.4$ (flight test data = symbols; model = dashed).

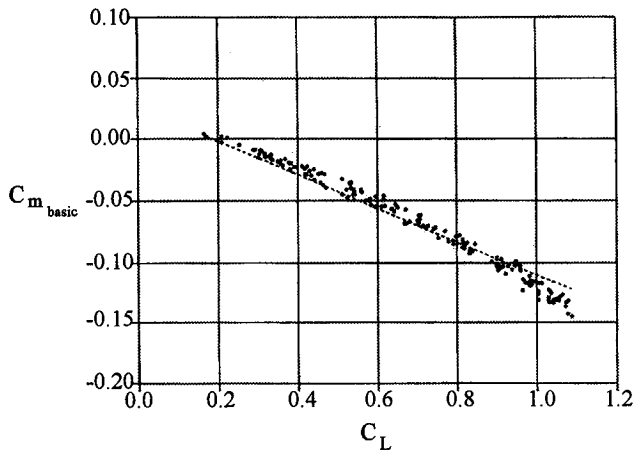

Fig. 7 Basic pitching moment for $M_0 = 0.4$ (flight test data = symbols; model = dashed).

substituted into Eqs. (12) along with the regression constants. Figure 5 shows a plot of $C_{L_{model}}$ superimposed on the same set of flight test data used in Fig. 3, where the number of data points has been reduced for plotting purposes. The data and model are reduced by subtracting the sum of the dynamic, control, and configuration terms [i.e., $a_3(\hat{q} + \partial\varepsilon/\partial\alpha\hat{\alpha}) + a_4\delta_H + a_5\delta_f + a_6\delta_f\alpha$], from both the model and the data. This is similar to that which would be observed in static wind-tunnel testing for $\delta_f = 0$ deg. Figures 6 and 7 show similar plots for $C_{D_{basic}}$ and $C_{m_{basic}}$, respectively.

Model Validation

Substituting Eqs. (12) into the longitudinal equations of motion[8] gives

$$\dot{U} = [(C_{L_{model}} \sin\alpha - C_{D_{model}} \cos\alpha)\bar{q}S + X_T]/m - g\sin\theta - qW$$

$$\dot{W} = -[(C_{L_{model}} \cos\alpha + C_{D_{model}} \sin\alpha)\bar{q}S + Z_T]/m + g\cos\theta + qU$$

$$\dot{q} = (C_{m_{model}}\bar{q}S\bar{c} + M_T)/I_{yy}$$

$$\dot{\theta} = q$$

where X_T, Z_T, M_T, and I_{yy} were computed by the engine model. If the modeled terms are accurate, then the propa-

gation of these equations using only the pilot inputs (i.e., δ_H and throttle) from a particular flight segment should reproduce that segment with minimal residual between simulation and the measured states.

Initialization of the Simulator

The simulator was initialized to a level trim flight condition using the nominal values of the states, δ_H, the altitude, δ_f, the inertial terms, and the thrust terms from a particular flight test. The trim point of the model was found using integral + derivative feedback of the altitude error to δ_H and proportional + derivative feedback of the velocity error to X_T. This was simply a stable autopilot that forced the altitude and airspeed to steady-state values. Successful execution provided biases (assumed to be from measurement errors) in α, θ, δ_H, and X_T that were used in the subsequent simulation. Biases in all other parameters were assumed to be zero.

Simulation

The simulation model was integrated at 20 Hz using only the pilot inputs corrected for biases. The α and θ responses are shown in Figs. 8 and 9, respectively. It was observed that the simulation accuracy was highly sensitive to the values of C_{L_0} and C_{m_0} in that those listed in Table 2 provided disparate results for each flight tested. Two causes for this come to mind. First, any terms erroneously neglected in the structure of Eqs. (12) during the identification would result in a modeling bias distributed throughout the remaining terms in the model. The trim point calculation would provide the measurement biases that in effect shifted this modeling bias to C_{L_0} and C_{m_0}. In order to circumvent this problem, an automatic model structure determination algorithm such as stepwise regression may be used. The reader is referred to Ref. 1. Second, the assumption of zero biases other than those identified in the trim point calculation may be suspect. Notwithstanding this, the values of C_{L_0} and C_{m_0} assigned for the simulation illustrated here were 0.001 and 0.035, respectively. These values are still very close to those shown in Table 2 and certainly the relative difference is within the accuracy of the test instrumentation.

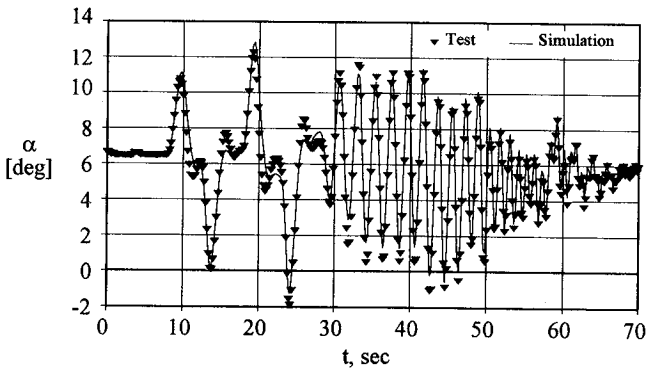

Fig. 8 Angle-of-attack simulation response comparison to flight test data (M_0 = 0.3).

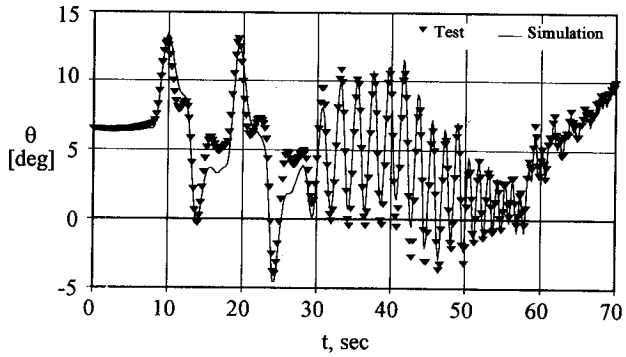

Fig. 9 Pitch attitude simulation response comparison to flight test data (M_0 = 0.3).

In testing the accuracy of a modeling scheme, the identified model should be compared to the data used to generate it. Conversely, in testing the model fidelity, the model should be compared to data not previously used in any identification attempts. The time responses of α and θ compared quite well with the data as shown in Figs. 8 and 9. The trim ($0 < t < 8$ s) and pitch doublet ($8 < t < 26$ s) portions had not been used in the identification. Other responses such as altitude and airspeed also showed good agreement. Note the attenuation at $t \approx 45$ s due to the increasing frequency of the δ_H (as was expected based on frequency response characteristics). During the frequency sweep δ_H was maintained at a nominally constant amplitude of oscillation. Only data having frequencies below that of the short period was used in the modeling. Yet for $t > 45$ s, the simulation compares nicely with the data.

Conclusions

The formulation of the mathematical model structure of the lift, drag, and pitching moment has been illustrated through the discussion of key theoretical applications such as the Prandtl–Glauert similarity transformation and the approximate nonlinear lift relationship at high angle of attack. The inclusion of the $\dot{\alpha}$ term was illustrated via the approximate stability derivatives C_{L_q}, C_{m_q}, $C_{L_{\dot{\alpha}}}$, and $C_{m_{\dot{\alpha}}}$. An appropriate grouping of these terms was suggested that allowed for their proper identification by eliminating the need to overcome the large correlation between q and $\dot{\alpha}$. The steps used in the parameter identification technique have been described revealing the iterative nature associated with a problem of this kind. Finally, the model was validated through simulation and showed excellent agreement with flight test data that had not previously been used in the model estimation.

References

[1]Draper, N. R., and Smith, H., *Applied Regression Analysis*, Wiley, New York, 1981, pp. 70–122, 307–311.

[2]"YAV-8B Simulation and Modeling. Volume 1: Aircraft Description and Program Summary," McDonnell Douglas Corp., NASA CR-170397, 1983.

[3]Anderson, L. C., and Vincent, J. H., "AV-8B System Identification Results: Low and High Speed Longitudinal Model," NATC CR N00421-81-C-0289, April 1984.

[4]Bach, R. E., Jr., and McNally, B. D., "A Flight-Test Methodology for Identification of an Aerodynamic Model for a V/STOL Aircraft," NASA TM 100067, March 1988.

[5]Bach, R. E., Jr., "State Estimation Applications in Aircraft Flight-Data Analysis," *A User's Manual for SMACK*, NASA RP-1252, March 1991.

[6]Pope, A., *Basic Wing and Airfoil Theory*, McGraw-Hill, New York, 1951, pp. 120–153.

[7]Kuethe, A. M., and Chow, C.-Y., *Foundations of Aerodynamics*, Wiley, New York, 1986, pp. 192–206.

[8]Etkin, B., *Dynamics of Flight-Stability and Control*, Wiley, New York, 1982, pp. 140–147, 239–246.

[9]Plaetschke, E., and Schulz, G., "Practical Input Signal Design," *Parameter Identification*, AGARD-LS-104, Oct. 1979, pp. 3-1–3-19.